*buildings*

MDPI

*Article*

# Mechanical Response Characteristics and Tangent Modulus Calculation Model of Expansive-Clay Unloading Stress Path

**Shilong Peng [1,2,3,*], Zhijun Li [1,2], Hua Cheng [1,2,3,4], Yuhao Xu [1,2], Ting Zhang [1,2] and Guangyong Cao [1,2,3]**

[1] Anhui Provincial Key Laboratory of Building Structure and Underground Engineering, Anhui Jianzhu University, Hefei 230601, China; lycheejun@stu.ahjzu.edu.cn (Z.L.); hcheng@ahu.edu.cn (H.C.); xyh@stu.ahjzu.edu.cn (Y.X.); zhangt@ahggzyjt.com (T.Z.); caogy@ahjzu.edu.cn (G.C.)
[2] College of Civil Engineering, Anhui Jianzhu University, Hefei 230601, China
[3] Engineering Research Center of Underground Mine Construction, Ministry of Education, Anhui University of Science and Technology, Huainan 232001, China
[4] School of Resources and Environmental Engineering, Anhui University, Hefei 230022, China
* Correspondence: psl@ahjzu.edu.cn

**Abstract:** As a special type of clay, expansive clay is widely distributed in China. Its characteristics of swelling and softening when meeting water and shrinking and cracking when losing water bring many hidden dangers to engineering construction. Expansive clay is known as "engineering cancer", and in-depth research on the unloading mechanical response characteristics and the unloading constitutive relationships of expansive clay is a prerequisite for conducting geotechnical engineering design and safety analysis in expansive-soil areas. In order to obtain the unloading mechanical response characteristics and the expression of the unloading tangent modulus of expansive clay, typical expansive clay in the Hefei area was taken as the research object, and triaxial unloading stress path tests were conducted. The stress–strain properties, microstructures, macro failure modes, and strength indexes of the expansive clay were analyzed under unloading stress paths. Through an applicability analysis of several classical soil strength criteria, an unloading constitutive model and the unloading tangent modulus expression of the expansive clay were constructed based on the Mohr–Coulomb (hereinafter referred to as "M-C") criterion, the Drucker–Prager (hereinafter referred to as "D-P") criterion, and the extended Spatial Mobilized Plane (hereinafter referred to as "SMP") criterion theoretical frameworks. The following research results were obtained: (1) The stress–strain curves of the three stress paths of the expansive clay were hyperbolic. The expansive clay showed typical strain-hardening characteristics and belonged to work-hardening soil. (2) Under the unloading stress paths, the soil particles were involved in the unloading process of stress release, and the failure samples showed obvious stretching, curling, and slipping phenomena in their soil sheet elements. (3) Under both unloading stress paths, the strength of the expansive clay was significantly weakened and reduced. Under the lateral unloading paths, the cohesive force ($c$) of the expansive clay was reduced by 32.7% and the internal friction angle ($\varphi$) was increased by 19% compared with those under conventional loading, while under the axial unloading path, $c$ was reduced by 63.5% and $\varphi$ was reduced by 28.7%. (4) For typical expansive clay in Hefei, the conventional triaxial compression (hereinafter referred to as "CTC") test, the reduced triaxial compression (hereinafter referred to as "RTC") test, and the reduced triaxial extension (hereinafter referred to as "RTE") test stress paths were suitable for characterization and deformation prediction using the M-C strength criterion, D-P strength criterion, and extended SMP strength criterion, respectively. (5) The derived unloading constitutive model and the unified tangent modulus formula of the expansive clay could accurately predict the deformation characteristics of the unloading stress path of the expansive clay. These research results will provide an important reference for future engineering construction in expansive-clay areas.

**Keywords:** expansive clay; constitutive model; unloading stress path; triaxial test; tangent modulus calculation model



**Citation:** Peng, S.; Li, Z.; Cheng, H.; Xu, Y.; Zhang, T.; Cao, G. Mechanical Response Characteristics and Tangent Modulus Calculation Model of Expansive-Clay Unloading Stress Path. *Buildings* **2024**, *14*, 2497. https://doi.org/10.3390/buildings14082497

Academic Editor: Eugeniusz Koda

Received: 12 July 2024
Revised: 31 July 2024
Accepted: 6 August 2024
Published: 13 August 2024

## 1. Introduction

Expansive clay is a special kind of clay with strong expansion, contraction, and over-consolidation that is widely distributed in more than 20 provinces in China, including Guangxi, Yunnan, Hubei, Anhui, Sichuan, Henan, Shandong, etc. Especially in arid and semi-arid areas, expansive clay in the shallow surface stratum is involved in the wet and dry cycle of rainfall and evaporation all year round, and it is unsaturated soil in its natural state [1,2]. Due to the development of internal cracks, its general engineering properties are poor, which has a great impact on construction projects, and it is known as "engineering cancer". A large number of studies [3,4] have shown that in the process of foundation pit excavation in an expansive-clay layer, the sidewalls and bottom soil of the foundation pit are in a state of "unloading" stress, and their strength and bearing capacity are significantly reduced by the excavation unloading effect. The soil in a pit is in an unstable state due to excavation unloading deformation and strength deterioration, frequently leading to the occurrence of serious engineering accidents such as deep foundation pit collapse and slope instability [5]. Therefore, when an underground structure support design is carried out in an expansive-clay layer, it is crucial to carry out a structural design and safety analysis of the foundation pit to fully consider the influence of the unloading effect on the unloading deformation and strength deterioration of the expansive clay [6], to deeply explore the unloading mechanical response characteristics, and to develop an unloading constitutive model of the expansive clay.

The stress path has an important influence on the mechanical response characteristics of soil, so the effects of stress paths should be fully considered when establishing a soil unloading constitutive model [7,8]. Since Lambe [9] proposed the concept of stress path correlation in the 1960s, scholars at home and abroad have carried out a series of studies on nonlinear and elastoplastic constitutive models of soil considering stress paths. In the study of nonlinear constitutive models of soil considering stress paths, since Duncan and Chang [10] put forward the nonlinear Duncan–Chang model in 1970, the subsequent constitutive model research in this field has mostly been based on improving and revising the Duncan–Chang model. Gao Zhenzhong [11] studied the stress–strain properties of silty soil under an unloading stress path. He put forward a nonlinear constitutive model that comprehensively considered strain softening, shear dilatancy (or shear shrinkage) properties, and unloading effects. He verified the correctness of this model through an experimental test of a volume change curve. Yin Deshun [12] deduced the calculation formulas of the Duncan–Chang model under axial and lateral unloading, which addressed the Duncan–Chang model's inability to consider the stress path. S. Goto [13] put forward a nonlinear model of an unloading stress path suitable for small-strain planes. The parameters of this model could be measured via indoor triaxial and shear-wave velocity tests. It was found that this model could accurately predict the small-strain behavior of soil under an unloading path. In 1963, Roscoe [14] established a constitutive model according to triaxial tests of reshaped clay with normal and weak consolidation (called the "Cam-clay model"). The subsequent elastoplastic models of soil considering stress paths were mostly based on the framework of the Cam-clay model [15]. In 1968, Roscoe and Burland [16] further modified the Cam-clay model, changing its yield surface trajectory into an ellipse, and obtained a modified Cam-clay model, which is widely used now. On the basis of the Cam-clay model, Robert Lo [17] adopted the Row dilatancy formula to reflect the shear dilatancy of soil. He combined this formula with the energy formula of the Cam-clay model, and a modified elastoplastic model was obtained to predict the stress–strain relationships of soils under unloading stress paths. Matsuoka [18] embedded the three-dimensional strength criterion (SMP criterion) into the modified Cam-clay model by transforming the stress method. He produced a three-dimensional model and further predicted the stress–strain properties of sandy soil and clayey soil under an unloading path condition. Yao Yangping [19,20] applied the SMP strength criterion to an elastoplastic model with double-yield surfaces to produce a three-dimensional model. He subsequently produced a three-dimensional model of the Tsinghua model [21]. Based on the stress path test results

of Fengpu sand, Lu Dechun [22] put forward a generalized nonlinear strength criterion by decomposing the stress path of sand. Then, he established an elastic–plastic constitutive model of soil stress paths based on the Cam-clay model. Zhang Kunyong [23], based on the Cam-clay model and drawing lessons from the modeling concepts of the Ohta–Sechiguchi model, established a three-dimensional elastoplastic constitutive model. This three-dimensional elastoplastic constitutive model reflects the stress–strain characteristics of soil excavation unloading under *K*0 consolidation conditions. As a kind of special clay with a wide distribution, the unloading deformation and strength properties of expansive clays are quite different from those of general clay. There have been fewer studies on the unloading stress path constitutive models of expansive clay. Therefore, it is of great guiding significance to explore the mechanical response characteristics of expansive clay under unloading paths and establish a constitutive model for engineering practice in expansive-clay areas.

In view of this, based on the automatic environmental triaxial test system (ETAS), this study took expansive clay in typical strata in Hefei as the research object, and a conventional triaxial compression (hereinafter referred to as "CTC") test, reduced triaxial compression (hereinafter referred to as "RTC") test, and reduced triaxial extension (hereinafter referred to as "RTE") test were carried out to analyze the failure modes. The stress–strain properties and strength indexes of the expansive clay were determined under unloading stress paths. Through an applicability analysis of several classical soil strength criteria, an unloading constitutive model of expansive clay was constructed, and a unified formula of the tangent modulus of expansive clay under an unloading stress path was obtained. These research results can provide an important reference for future engineering construction in expansive-clay areas.

## 2. Stress Path Analysis of Unloading Soil in Foundation Pit Excavation

For common narrow and long foundation pits, the size in one direction is much larger than that in the other, and the stress state of the foundation pit can be simplified as a two-dimensional plane strain problem. In the process of foundation pit excavation, the stress path of the soil at the bottom and on the side of the foundation pit is constantly changing. It can be roughly divided into two areas according to the position and stress state of the soil in the pit [24,25]: ① The first area is a passive area at the bottom of the foundation pit, where the axial unloading of the soil is greater than the horizontal unloading. It can be idealized that the horizontal stress remains constant and the vertical stress decreases (axial unloading). ② The second area is the lateral active area of the foundation pit, where the horizontal unloading of the soil is greater than the axial unloading. In the idealized situation, the vertical stress is constant and the horizontal stress is reduced (lateral unloading), as shown in Figure 1.

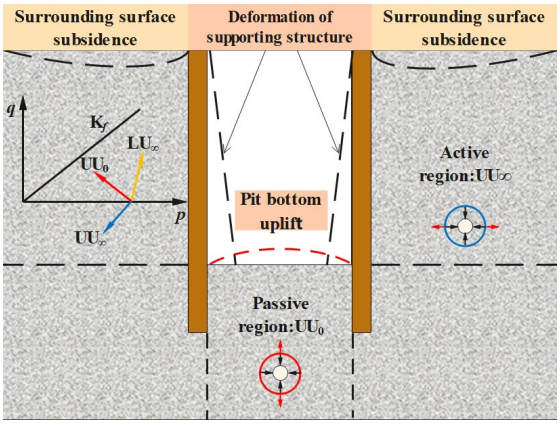


**Figure 1.** Stress state and path division of soil in foundation pit.

## 3. Unloading Stress Path Tests on Expansive Clays

### *3.1. Soil Sample*

Hefei City, Anhui Province, is a typical area of expansive clay distribution in China, and the expansive clay in this area is widely distributed in the first terrace of the Nanfei River and the undulating plain landform of Jianghuai, as shown in Figure 2. According to a relevant investigation report [26], a test showed that the mineral composition of the expansive clay of the Upper Pleistocene Qizui Formation (Q3q) in the undulating Jianghuai plain is mainly illite, which contains ferromanganese nodules and is expansible. The expansive clay used in this experiment was excavated from a foundation pit in Hefei, and the drilling depth was 14~20 m.

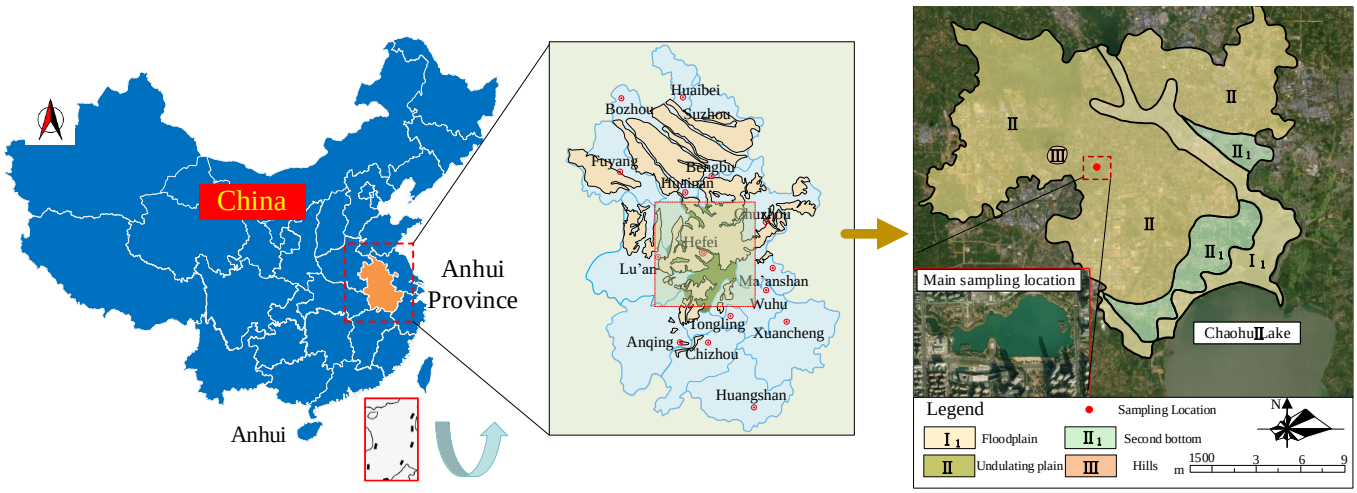


**Figure 2.** A distribution map of the expansive clay in Anhui Province and the main sampling location for this article.

According to the basic physical properties of 201 groups of soil samples obtained from geotechnical tests, such as the boundary moisture content and free-expansion rate, the average values of the basic physical parameters of all soil samples were calculated [27], as shown in Table 1.

**Table 1.** Indicators of basic physical properties of soil samples for testing.

| Natural Moisture Content $\omega$ (%) | Dry Density $\rho_d$ (g/cm$^3$) | Void Ratio $e$ | Plastic Limit $\omega_P$ (%) | Liquid Limit $\omega_L$ (%) | Plasticity Index $I_P$ | Free-Expansion Rate $\delta_{ef}$ (%) |
|---|---|---|---|---|---|---|
| 23.4 | 1.73 | 0.743 | 21.3 | 39.6 | 18.3 | 47.1 |

Using the liquid limit as the abscissa and the plasticity index as the ordinate, and employing consistency states to partition the data points, a plasticity chart of the expansive clay in Hefei was obtained (as shown in Figure 3). The light gray area above line A in the plasticity chart represents the clayey soil zone, while the dark gray area below line A represents the silty soil zone. These two zones are divided into low-liquid-limit, medium-liquid-limit, and high-liquid-limit regions by lines B and C. From an analysis of Figure 3, it could be determined that the expansive clay in Hefei fell into the category of medium- to high-liquid-limit clayey soil and that the plasticity index ($I_P$) was positively correlated with the liquid limit ($\omega_L$) $I_P = -0.011\omega_L^2 + 1.434\omega_L - 22.083$.

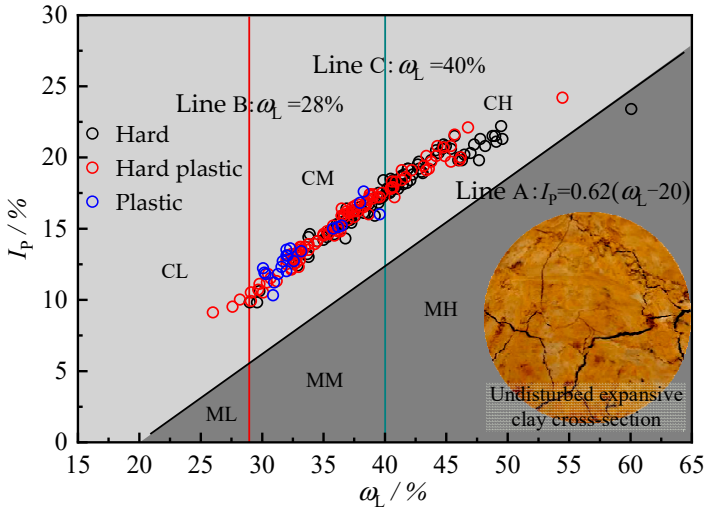


**Figure 3.** Plasticity chart for the compaction state of expansive clay.

According to the analysis in Table 1, the free-expansion rate of the Hefei expansive clay was between 40% and 65%, and the plasticity index was between 18 and 28, which indicated its weak expansibility. The sample preparation method referred to the Standard for Geotechnical Test Methods (GB/T 50123-2019, Chinese Standard) [27], with a size of Φ50 mm × 100 mm, a moisture content of 15%, and a dry density of 1.83 g/cm$^3$.

### *3.2. Test Apparatus*

The test apparatus was an automatic environmental triaxial test system (ETAS) (Figure 4) from the School of Civil Engineering, Anhui Jianzhu University. This system could perform back pressure saturation, B value detection, the standard triaxial test, and the stress path test. In this study, the Advanced Load and Standard Triaxial modules were adopted for the unloading stress path test. These modules could accurately carry out the process of sample consolidation and the triaxial loading test, and GDSLAB could collect data in real time. The specific parameters of the ETAS are shown in Table 2.

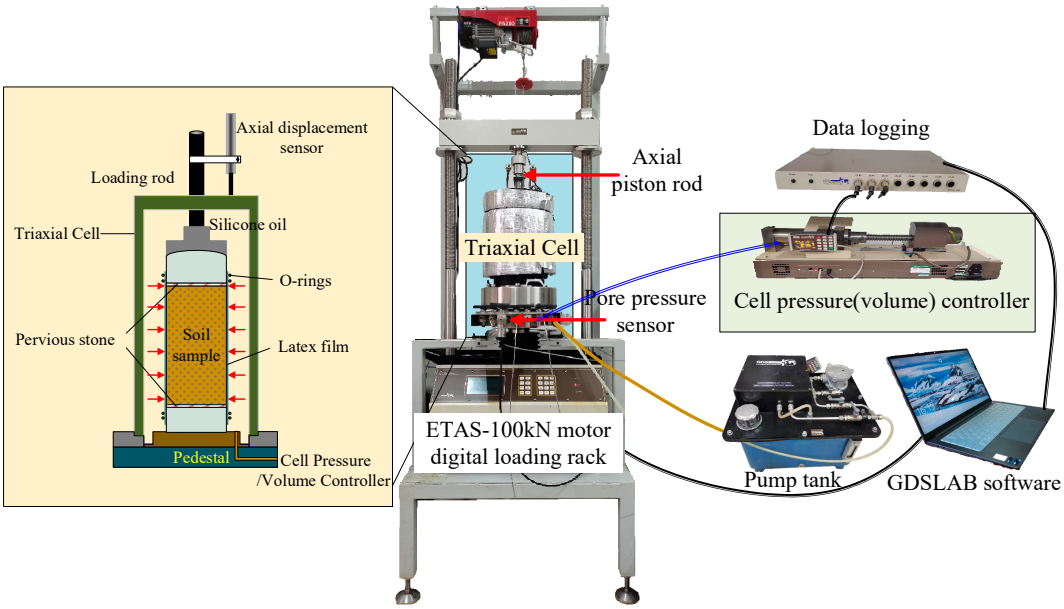


**Figure 4.** Automated environmental triaxial test system (ETAS).

**Table 2.** Equipment parameters.

| Maximum Vertical Load kN | Maximum Cell Pressure MPa | Load Sensor Range kN | Pore Pressure Sensor Range MPa | Axial Displacement Sensor Range mm |
|---|---|---|---|---|
| 100 | 32 | 100 | 32 | ±25 |

### *3.3. Sample Program*

In order to explore the unloading mechanical response characteristics of the expansive clay, three stress path triaxial test schemes [28] were designed according to the stress zoning of soil in a foundation pit, namely, CTC, RTC, and RTE. The cell pressure in the test consolidation stage adopted the isotropic loading mode, and the consolidation cell pressure was $\sigma_c$. The specific test scheme was as follows:

(1) The CTC test adopted displacement-controlled loading with an axial loading rate of 0.2 mm/min.
(2) The RTC test adopted stress-controlled unloading. The vertical stress remained unchanged during the shearing process, while the lateral stress decreased at an unloading rate of 0.2 kPa/min until the shearing was completed.
(3) The RTE test adopted stress-controlled unloading. The lateral stress remained unchanged, while the axial stress decreased at an unloading rate of 0.2 kPa/min until the shearing was completed.

The triaxial loading (unloading) test program is shown under different stress paths in Table 3.

**Table 3.** Triaxial loading (unloading) test program under different stress paths.

| Stress Path Types | Loading (Unloading) Methods | Consolidation Stress/kPa | Simulated Soil Position | Shearing Rate |
|---|---|---|---|---|
| CTC | $LU_\infty$ | 100, 200, 300, 400 | conventional axial loading | load 0.2 mm/min |
| RTC | $UU_\infty$ | 300, 400, 500, 600 | passive zone | unload 0.2 kPa/min |
| RTE | $UU_0$ | 200, 300, 400 | active zone | |

Note: In the stress path labeling, the letters in the front row represent axial stress loading (unloading) and the letters in the back row represent radial stress loading (unloading), where '*L*' indicates loading and '*U*' indicates unloading. The subscript is numerically equal to the absolute value of the ratio of axial stress to radial stress variation.

## 4. Analysis of Test Results

### *4.1. Stress–Strain Curves and Macroscopic Characterization of Shear Failure*

Figures 5–7 are schematic diagrams of the stress–strain curves and shear failure characteristics of the expansive clay under the three stress paths of CTC, RTC, and RTE, respectively. Figure 8 shows the typical stress–strain properties of the three stress paths with an initial consolidation pressure ($\sigma_c$) of 400 kPa. From an analysis of Figures 5–8, it can be seen that the stress–strain curves of the three stress paths of the expansive clay with different stress levels were hyperbolic. The initial tangent modulus increased with an increase in the initial consolidation stress, which is typical of strain-hardening properties. The expansive clay was a work-hardening soil, as its compressibility was not affected by the stress paths.

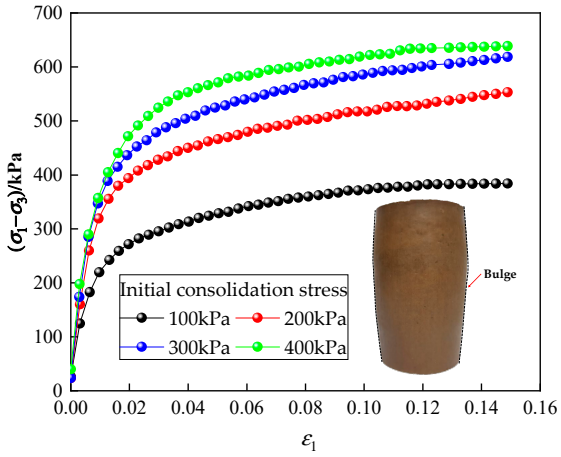


**Figure 5.** CTC stress–strain curve and failure modes.

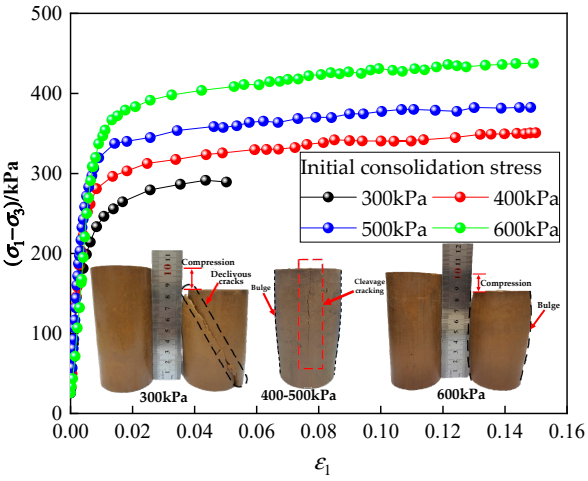


**Figure 6.** RTC stress–strain curve and failure modes.

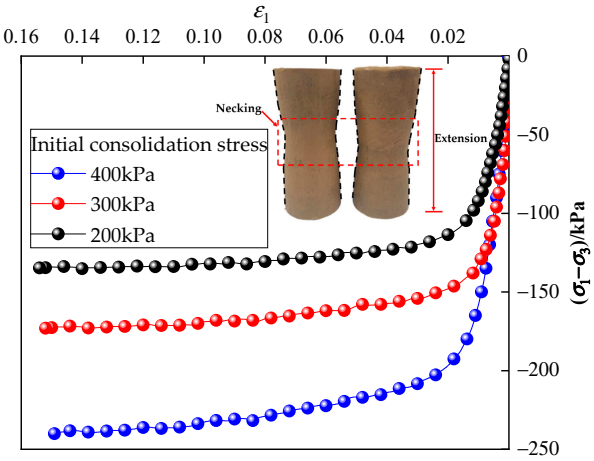


**Figure 7.** RTE stress–strain curve and failure modes.

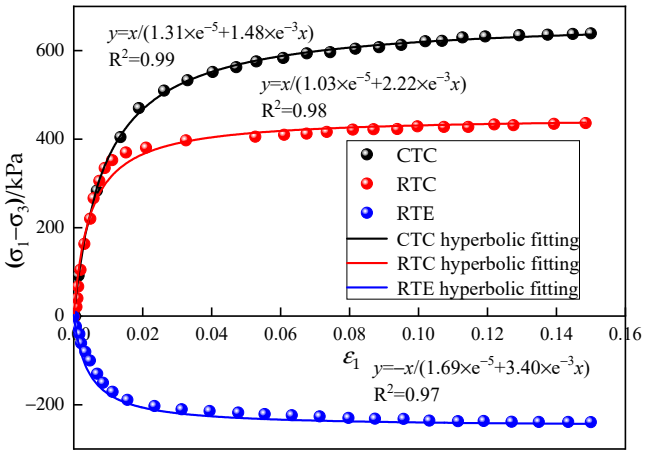


**Figure 8.** Stress–strain curve when $\sigma_3 = 400$ kPa.

The stress–strain curves of CTC, RTC, and RTE had significant differences in their growth rates, peak growth values, and failure modes. The stress–strain curve of CTC was relatively smooth as a whole, and it tended to slow down after the axial strain reached 9%. The sample showed spindle-like bulging failure. Due to the end-compression shear effect, there were many fine cracks at both ends, but there was no overall oblique shear fracture surface [29]. The RTC curve was mutable. The deviatoric stress approached its peak after the axial strain reached 2%, and then tended to be stable. As the initial consolidation confining pressure increased, the specimen gradually transitioned from shear failure to lateral bulging failure during fracture. The overall trend in the RTE curve was similar to that of the RTC curve, and it was also mutable. When the axial strain was less than 2%, the deviatoric stress reached its peak. The specimen was dumbbell-shaped and collapsed in the middle. At the same time, the peak strength of the Hefei expansive clay was significantly lower under the RTC and RTE unloading paths compared with the CTC path. This strength attenuation was most obvious in the RTE unloading path, followed by the RTC path.

Affected by the lag of the unloading deformation of the expansive clay, the unloading strain of RTC and RTE was small in the initial stage of unloading. When the deviatoric stress reached a certain unloading ratio, the strain suddenly increased, producing a curve growth rate that was significantly different from that observed during CTC. These kinds of unloading deformation lag and abruptness also manifest in practical engineering, as soil usually suffers unloading damage abruptly. This brings great risks to the construction of expansive-clay unloading engineering.

### *4.2. Microscopic Properties of Shear Failure*

Figures 9 and 10 show scanning microstructure diagrams of the three stress paths of the shear failure samples in transverse and longitudinal sections, respectively, when the initial consolidation cell pressure ($\sigma_c$) was 300 kPa. Due to the weak mechanical connections between the illite minerals in the Hefei expansive clay, when shear failure occurred, the sheet mineral aggregates were petal-shaped, curled, wrinkled, and warped, and they had specific directional arrangement properties. With increases in the curling and sliding of the sheet structure of the clay minerals, the strength of the soil gradually deteriorated. This phenomenon was consistent with the unloading strength attenuation of the expansive clay.

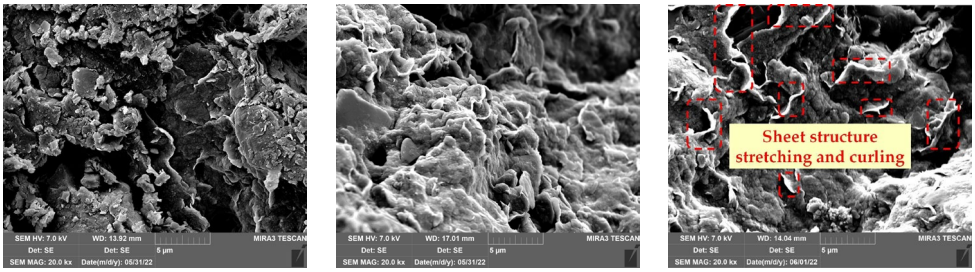


(**a**) CTC (**b**) RTC (**c**) RTE

**Figure 9.** Transverse section of failure sample of expansive clay.

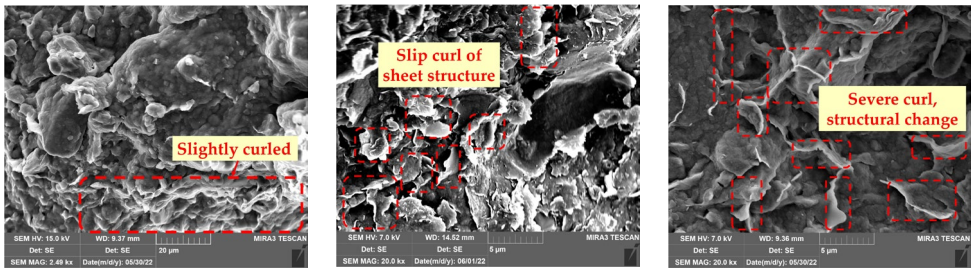


(**a**) CTC (**b**) RTC (**c**) RTE

**Figure 10.** Longitudinal section of failure sample of expansive clay.

The CTC sample was subjected to the combined effects of radial cell pressure constraint and axial pressure loading compression, and the clay particles were compacted and tended to be densely arranged. At the same time, the bulging in the middle of the sample during failure caused the soil particles to slide, which resulted in the clay particles having a certain degree of directional arrangement in the cross-section. The micro-units in the longitudinal section were compacted by the loading action, which restricted the curling of the sheet particles, preventing overall warping. Only slight warping could be observed at the edges. The soil particles in the RTC and RTE samples were released by the unloading effect. The soil particles in the transverse section of the shear failure sample were not oriented. However, there were obvious sheet element stretching and curling phenomena in the transverse section of the RTE sample. Due to the decrease in the lateral binding force during the RTC test, the soil particles were easier to move, and the sheet elements of the longitudinal soil slid and curled, which led to the shear failure behavior of the expansive clay. During the RTE test, the sheet structure of the soil was seriously curled, and the structure changed. The directional arrangement was obvious, which led to the necking and tensile failure of the soil.

### *4.3. Analysis of Change Rule of Shear Strength Index*

Through an analysis of the stress–strain properties of the expansive clay under the three stress paths, it was found that the strength of the expansive clay significantly deteriorated and decayed under unloading. The strength indexes of the three stress paths of the expansive clay were obtained, as shown in Table 4.

By comparing the strength indexes of the expansive clay under the three stress paths, it was found that in the RTC and RTE tests, the $c$ of the expansive clay was reduced by 32.7% and 63.5%, respectively, compared with the CTC test. During the RTC test, the initial consolidated and compacted clay particles slipped twice under lateral unloading, which led to weakening of the cementing force between the clay particles and a decrease in $c$. During the RTE test, the soil sample was in a state of stretching and extrusion. The clay particles were separated by the stretching, which led to a minimal $c$ value. During the RTC test, due to the dual effects of lateral unloading and axial compression, the friction and occlusion between the clay elements were strengthened, which led to a 19% increase in

the $\varphi$ in the expansive clay compared with that under conventional loading. During axial unloading, the unloading effect reduced the sliding friction strength and biting friction strength between particles, which led to a 28.7% reduction in $\varphi$ compared with the CTC test.

**Table 4.** Test results and strength indicators of expansive clay.

| Stress Paths | Maximum Principal Stress $\sigma_1$/kPa | Medium Principal Stress $\sigma_2$/kPa | Minimum Principal Stress $\sigma_3$/kPa | Failure Deviatoric Stress ($q_f$=$\sigma_1-\sigma_3$)/kPa | Internal Friction Angle $\varphi$/° | Cohesive Force $c$/kPa |
|---|---|---|---|---|---|---|
| CTC | 499.18 | 100 | 100 | 399.18 | 19.1 | 101.7 |
| | 711.55 | 200 | 200 | 511.55 | | |
| | 925.81 | 300 | 300 | 625.81 | | |
| | 1067.68 | 400 | 400 | 667.68 | | |
| RTC | 300 | 4.97 | 4.97 | 295.03 | 22.73 | 68.4 |
| | 400 | 49.48 | 49.48 | 350.52 | | |
| | 500 | 112.86 | 112.86 | 387.14 | | |
| | 600 | 184.80 | 184.80 | 415.20 | | |
| RTE | 200 | 200 | 65.27 | 134.73 | 13.64 | 37.1 |
| | 300 | 300 | 126.92 | 173.08 | | |
| | 400 | 400 | 185.40 | 214.60 | | |

$c$ and $\varphi$ are the two most important basic parameters in geotechnical engineering calculations, and their accuracy is directly related to the stability and deformation analysis of a foundation pit. When a foundation pit is unloaded in the expansive-clay layer and the soil is in an unloading state, its strength is greatly reduced. If the strength index of the CTC test is used for engineering structure design and construction, the influence of the unloading stress path caused by excavation on the soil parameters is ignored. This easily leads to irrational engineering design and increases the risk of construction. Therefore, it is of great significance to determine the soil parameters and strength index of an unloading stress path and to carry out structural design to ensure the safety of a foundation pit.

## 5. Applicability Analysis of Strength Criterion for Expansive Clay under Unloading Path

In engineering practice, for the calculation of an expansive-clay layer, the standard practice is to invert the M-C strength criterion through the CTC test and then establish a loading constitutive model using this criterion. From the analysis of the unloading stress path test of the expansive clay, it could be seen that the mechanical response characteristics of the expansive clay were significantly different under the RTC and RTE unloading stress paths from those during the CTC test. In order to establish an unloading constitutive model of the expansive clay, it was necessary to compare and analyze the applicability of various classical strength criteria according to the test results of the unloading stress path. Then, unloading constitutive models suitable for the different stress paths of the expansive clay were established.

Table 5 shows four strength criteria commonly used in soil mechanics. In this section, the initial average principal stress $(p)$ and the failure deviatoric stress $(q_f)$ were obtained from the unloading stress path test results. The expression of $f(p, q, \theta) = 0$, under the theoretical framework of the four strength criteria, was derived for the applicability analysis of the strength criteria.

From the analysis in Table 5, it can be seen that the influence of $p$ is considered in the four strength criteria, which reflect the compressibility of the soil, while the D-P strength criterion does not consider the influence of the stress Lode angle $(\theta)$. Based on their deformation properties, the three kinds of stress path triaxial tests designed in this paper can be divided into triaxial compression tests (CTC and RTC) and a triaxial extension test (RTE). For the CTC and RTC tests, $\sigma_1 > \sigma_2 = \sigma_3$ ($\sigma_1$ is axial stress, while $\sigma_2$ and $\sigma_3$ are radial stress), and the stress Lode angle is $\theta = -30°$. In the RTE test ($\sigma_1$ and $\sigma_2$ are radial stresses, while $\sigma_3$ is axial stress), the stress Lode angle is $\theta = 30°$. By substituting the

test results of the unloading stress path in Table 4 into the four expressions of the strength criterion ($f(p, q, \theta) = 0$), as shown in Table 5, the values of failure deviatoric stress of the expansive clay were compared under different strength criteria. They were compared with the experimentally measured values (among them, the applicability of the extended SMP criterion for predicting the strength of expansive clay was analyzed by comparing the octahedral shear stress value ($\tau_8$) of the failure stresses with the $\tau_{8SMP}$ calculated using the extended SMP criterion for validation [33]). The results are shown in Figure 11.

**Table 5.** Strength criteria and parameters.

| Strength Criteria | $\pi$-Plane Expression | Strength Parameters | |
|---|---|---|---|
| Mohr–Coulomb [30] | $p\sin\varphi - \frac{1}{\sqrt{3}}q(\frac{1}{\sqrt{3}}\sin\theta\sin\varphi + \cos\theta) + c\cos\varphi = 0$ | $c$ | $\varphi$ |
| Drucker–Prager [31] | $q - 3\sqrt{3}\alpha_m p - \sqrt{3}k_m = 0$ | $\alpha_m$ | $k_m$ |
| Generalized Tresca [30] | $\sqrt{J_2}\cos\theta - k_t - \frac{1}{2}\alpha_1 I_1 = 0$ | $\alpha_1$ | $k_t$ |
| Extended SMP [32] | $J_2 - \frac{B(k-3)I_1}{2\sqrt{3k}}g(\theta) = 0,$ $B = \sqrt{k^2(k-9)/(k-3)^3},$ $g(\theta) = 1/\sin\left(\frac{\pi}{3} + \frac{1}{3}\sin^{-1}(B\sin\ 3\theta)\right)$ | $k$ | |

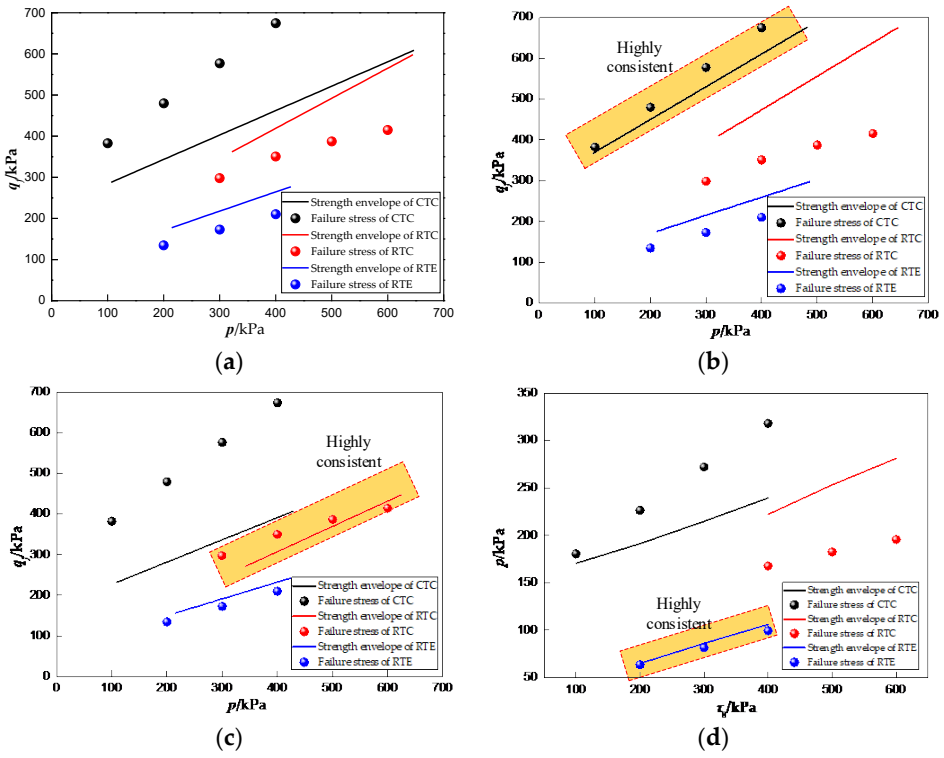


**Figure 11.** Strength criterion applicability analysis: (**a**) Generalized Tresca strength criterion applicability analysis; (**b**) M-C strength criterion applicability analysis; (**c**) D-P strength criterion applicability analysis; (**d**) Extended SMP strength criterion applicability analysis.

Taking the failure stress prediction error as a measure, it can be concluded that the M-C strength criterion was more accurate in predicting the strength of the expansive clay under the CTC path. The actual failure values were highly consistent with the theoretical values. Because the M-C strength criterion could not consider the deterioration effect of unloading on soil strength under the RTC and RTE paths, the calculation results of failure strength were too large and could not meet the calculation accuracy requirements of the unloading engineering of expansive clay. As a theory developed from the maximum shear

stress theory of metallic materials, the generalized Tresca criterion had poor prediction accuracy for the three stress path strengths of the expansive clays due to its own limitations. Neither the D-P criterion nor the generalized Tresca criterion could predict the failure stress value of the expansive clay under the CTC and RTE stress paths. The theoretical value was far lower than the measured value. The calculated value of the D-P criterion under the RTC unloading path was in good agreement with the stretching failure strength of the expansive clay. This shows that the D-P strength criterion could accurately predict the failure strength of the RTC path of the expansive clay. The extended SMP strength criterion was applicable to the strength prediction of the expansive clay under the three stress paths. The error between the octahedral failure stress calculated using the extended SMP criterion and the test value under the RTE unloading path was less than 6%, and the prediction effect was excellent. The priority of the applicability of the four strength criteria under the different stress paths is shown in Table 6, based on comprehensive analysis.

**Table 6.** Priority of applicability of four strength criteria.

| Stress Paths | Strength Criterion Applicability Grade |
|---|---|
| CTC | M-C > extended SMP > generalized Tresca > D-P |
| RTC | D-P > extended SMP > generalized Tresca > M-C |
| RTE | extended SMP > D-P = generalized Tresca = M-C |

To sum up, with regard to the expansive clay in the Hefei area, the most applicable strength criterion under the CTC path is the M-C strength criterion. The failure strength under the RTC path can be predicted using the D-P criterion, while the failure strength under the RTE path can be predicted using the extended SMP criterion.

## 6. Discussion of Unloading Constitutive Model of Expansive Clay

Studying the constitutive model of rock and soil mass is a key problem in the field of geotechnical engineering that directly affects the safety of engineering structure design. It is the foundation for establishing a constitutive model of rock and soil mass to describe the stress–strain behavior and the tangent modulus [34]. Expansive clay is known as "engineering cancer", and in-depth research on the unloading constitutive relationships of expansive clay is a prerequisite for conducting geotechnical engineering design and safety analysis in expansive-soil areas.

### *6.1. Analysis of Unloading Constitutive Model of Expansive Clay*

In 1970, Duncan and Chang combined the Kondner hyperbolic stress–strain relationship and the M–C criterion [10] to propose the tangent modulus of elasticity under loading conditions. They established the Duncan–Chang model based on isobaric consolidation CTC tests under the M–C criterion framework. The Duncan–Chang model is widely used in stress–deformation analysis, geotechnical engineering simulation, and geotechnical engineering design calculation because it is concise and intuitive and can better reflect the nonlinear characteristics of soil. However, with the continuous expansion of the scale of underground construction in China, underground spaces are gradually becoming closer to sensitive buildings and numerous underground pipelines. Due to the instability of underground rock and soil mass, the construction environment is becoming more and more complicated, and the accuracy of the Duncan–Chang model in predicting stratum deformation is gradually decreasing. For one thing, the Duncan–Chang model is a nonlinear incremental elastic model. Although a deformation modulus is introduced to represent the irreversible deformation of soil, it is different from the elastic–plastic model and cannot reflect the complex stress path. For another, the parameters of the Duncan–Chang model are determined by CTC tests, which are inconsistent with the unloading stress route of underground engineering. Therefore, due to the limitation of its theoretical basis, the Duncan–Chang model has many inherent and insurmountable calculation defects, and

there are sometimes great errors when describing stress–strain curves with simple hyperbolas, which lead to great differences between the calculated results of a tangent modulus and the actual results.

Experts and scholars have revised the parameters of the hyperbolic stress–strain formula considering the impact of the stress path [12]. However, they have not fully considered the effects of different unloading stress paths and strength criteria on the tangent modulus within the model. Based on the aforementioned test results of the unloading stress path of the expansive clay and the applicability analysis of the strength criteria, it is known that the unloading deformation of the foundation pit sidewalls and bottom soil of the expansive clay pit cannot be characterized using the M-C strength criterion. The applicability of the existing Duncan–Chang model and its related revised models for representing the tangent modulus of expansive clay needs further research and discussion. In view of this, establishing a unified formula for calculating the tangent modulus for the different unloading positions of the expansive clay pit has important theoretical significance for the structural design and safety analysis of the pit.

### *6.2. Calculation Model of Tangent Modulus of Expansive Clay under Unloading Path*

#### 6.2.1. Model Construction Ideas

In 1963, Kondner [35] proposed a hyperbolic formula to fit the stress–strain curve $(\sigma_1 - \sigma_3) \sim \varepsilon_1$ based on a large number of stress–strain curves of triaxial tests, that is, a hyperbolic model:

$$\frac{\varepsilon_1}{(\sigma_1 - \sigma_3)} = a + b\varepsilon_1 \tag{1}$$

In this formula, $\sigma_1$ is the axial stress; $\sigma_3$ is the radial stress; $\varepsilon_1$ is the axial strain; and $a$ and $b$ are parameters of the model-fitting curve.

Duncan and Chang [10] put forward the concept of the failure ratio ($R_f$) on the basis of the Kondner hyperbola model, and based on the M-C strength criterion, constructed a widely used incremental elastic model, that is, the Duncan–Chang model:

$$E_t = E_i \left[1 - \frac{R_f(\sigma_1 - \sigma_3)(1 - \sin\phi)}{2\sigma_3 \sin\phi + 2c\cos\phi}\right]^2, \tag{2}$$

In this formula, $(\sigma_1 - \sigma_3)$ is the deviatoric stress on the soil, and the failure stress of the soil under the initial consolidation pressure can be calculated using the M-C strength criterion.

Shao Dongchen [36] defined $S = (\sigma_1 - \sigma_3)/(\sigma_1 - \sigma_3)_f$ and regarded $S$ as the stress level parameter of soil. From the analysis of Formula (2), it can be seen that $S$ increases gradually with an increase in the deviatoric stress on the soil, and the tangent modulus ($E_t$) of the soil decreases accordingly, which accords with the concept that $E_t$ decreases with an increase in deviatoric stress. Therefore, the tangent modulus of the Duncan–Chang model is regarded as the initial tangent modulus reduction, and the reduction is controlled by $S$. The accuracy of the reduction coefficient determines the accuracy of the Duncan–Chang model in calculating the tangent modulus of the soil.

The traditional Duncan–Chang model is a soil constitutive model constructed under the framework of the M-C theory, and $E_t$ can only be predicted when the failure stress of the soil meets the M-C strength criterion. Based on the applicability analysis of the soil strength criterion under the unloading stress path of the expansive clay, it is known that the Duncan–Chang model based on the M-C strength criterion can be used to calculate the $E_t$ of expansive clay under CTC loading. However, the M-C strength criterion is not suitable for failure stress calculation under the RTC and RTE stress paths. Therefore, the D-P strength criterion and the extended SMP strength criterion should be introduced into the RTC and RTE stress paths of expansive clay to establish unloading constitutive models of expansive clay.

6.2.2. Establishment of Calculation Model for Unloading Tangent Modulus

From the above analysis, it can be seen that the D-P criterion has high accuracy in predicting the failure strength of expansive clay under the RTC path. According to the D-P strength criterion, expansive clay under the RTC path can be described using the following formula:

$$(\sigma_1 - \sigma_3)_f^{D-P} = 6(\sigma_3 \sin\varphi + c\cos\varphi)/(3 + \sin\varphi), \tag{3}$$

The complete form of the tangent modulus based on the D-P strength criterion of expansive clay under the RTC path can be obtained by substituting Formula (3) into Formula (2).

$$E_t^{D-P} = E_i\left[1 - \frac{R_f(\sigma_1 - \sigma_3)(3 + \sin\varphi)}{6\sigma_3 \sin\varphi + 6c\cos\varphi}\right]^2, \tag{4}$$

The introduction of the extended SMP criterion under the RTE path is significantly different from the D-P intensity criterion under the RTC path. As a nonlinear strength criterion, the extended SMP criterion features an asymmetrical strength curve on the $\pi$-plane, while the D-P criterion is circular in the $\pi$-plane, and its shape is not affected by the Lode angle ($\theta$). In order to introduce the extended SMP criterion into the Duncan–Chang model, we refer to the transformation stress space method proposed by Matsuoka H [18]. The extended SMP criterion is endowed with characteristics similar to the D-P criterion in the new stress space, and thus, the unloading constitutive model of expansive clay under the RTE path is established.

The transformed stress space requires the following transformation towards stress:

$$\widetilde{\sigma}_{ij} = p\delta_{ij} + \frac{q_c}{q}(\sigma_{ij} - p\delta_{ij}), \tag{5}$$

In this formula, $\widetilde{\sigma}_{ij}$ is the stress in the transformed stress space; $\sigma_{ij}$ is the stress in the original stress space; $p$ and $q$ are the average principal stress and shear stress; and $q_c$ is the deviatoric stress calculated using the extended SMP criterion.

The transformed stress process is shown in Figure 12. The stress points on the extended SMP criterion are mapped to the D-P criterion in the new stress space by means of stress transformation, that is, the process of changing stress point A to A* and stress point B to B* in the diagram, where $l_0$ is the vector diameter in the new stress space.

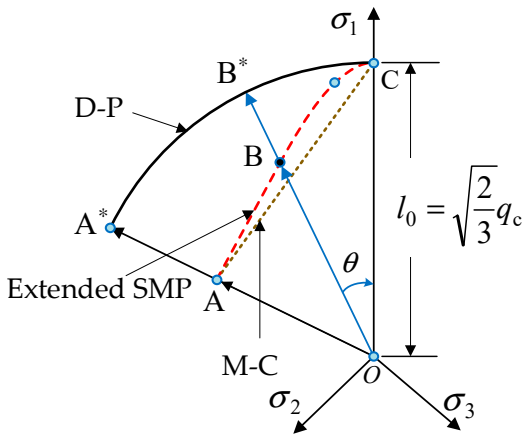


**Figure 12.** Schematic diagram of transformation stress.

According to the extended SMP criterion expression,

$$q_c = \frac{\hat{I}_1\hat{I}_2 - 9\hat{I}_3 + 3\sqrt{(\hat{I}_1\hat{I}_2 - \hat{I}_3)(\hat{I}_1\hat{I}_2 - 9\hat{I}_3)}}{4\hat{I}_2}. \tag{6}$$

According to the relationship between the vector diameter and the deviatoric stress ($q$) in the plane in Figure 12,

$$l_0 = \sqrt{\frac{2}{3}}\frac{\hat{I}_1\hat{I}_2 - 9\hat{I}_3 + 3\sqrt{\left(\hat{I}_1\hat{I}_2 - \hat{I}_3\right)\left(\hat{I}_1\hat{I}_2 - 9\hat{I}_3\right)}}{4\hat{I}_2}, \tag{7}$$

where $l_0$ is equivalent to the deviatoric stress $(\sigma_1 - \sigma_3)$ on the soil in the original Duncan–Chang model. The $l_f$ corresponding to $(\sigma_1 - \sigma_3)$ in a certain state can be calculated using Formula (7). Based on the extended SMP criterion in the transformed stress space, the limit value ($l_f$) of $l_0$ is

$$l_f = \sqrt{\frac{2}{3}}\frac{6\sin\varphi}{3 + \sin\varphi}\hat{\sigma}_3, \tag{8}$$

where $l_f$ is equivalent to the failure stress value $(\sigma_1 - \sigma_3)_f$ of the soil in the original Duncan–Chang model, and $S' = \frac{l_0}{l_f}$ is defined as the reduction factor in the extended SMP unloading constitutive model.

$$E_t^{SMP} = E_i\left[1 - \frac{R_f l_0}{l_f}\right]^2, \tag{9}$$

By substituting Formulas (7) and (8) into Formula (9), we can obtain

$$E_t^{SMP} = E_i\left[1 - \frac{R_f(3 + \sin\varphi)\left[\hat{I}_1\hat{I}_2 - 9\hat{I}_3 + 3\sqrt{\left(\hat{I}_1\hat{I}_2 - \hat{I}_3\right)\left(\hat{I}_1\hat{I}_2 - 9\hat{I}_3\right)}\right]}{24\hat{I}_2\hat{\sigma}_3\sin\varphi}\right]^2, \tag{10}$$

Formula (10) is the complete form of the tangent modulus of the unloading constitutive model of expansive clay based on the extended SMP strength criterion. According to Formula (10), the lateral stress ($\sigma_3$) under the RTE path is constant. By substituting a certain RTE unloading process into Formula (10), the tangent modulus under a certain deviatoric stress can be obtained.

From Formulas (2), (4), and (10), a unified formula for the unloading constitutive tangent modulus of expansive clay can be obtained based on the variation conditions of the major and minor principal stresses in the three stress paths:

$$E_t = E_i\begin{cases}\left[1 - \frac{R_f(\sigma_1-\sigma_3)(1-\sin\varphi)}{2\sigma_3\sin\varphi + 2c\cos\varphi}\right]^2 & \Delta\sigma_1 > 0, \Delta\sigma_3 = 0, \sigma_1 > \sigma_3 \\ \left[1 - \frac{R_f(\sigma_1-\sigma_3)(3+\sin\varphi)}{6\sigma_3\sin\varphi + 6c\cos\varphi}\right]^2 & \Delta\sigma_1 = 0, \Delta\sigma_3 > 0, \sigma_1 > \sigma_3 \\ \left[1 - \frac{R_f(3+\sin\varphi)\left[\hat{I}_1\hat{I}_2 - 9\hat{I}_3 + 3\sqrt{\left(\hat{I}_1\hat{I}_2 - \hat{I}_3\right)\left(\hat{I}_1\hat{I}_2 - 9\hat{I}_3\right)}\right]}{24\hat{I}_2\hat{\sigma}_3\sin\varphi}\right]^2 & \Delta\sigma_1 > 0, \Delta\sigma_3 = 0, \sigma_1 < \sigma_3\end{cases}, \tag{11}$$

### *6.3. Verification of Tangent Modulus*

In order to verify the accuracy of the unloading constitutive model of expansive clay, the theoretical value of the tangent modulus was calculated using the unified formula for the tangent modulus of expansive clay. Then, we compared and analyzed the results with the actual measurements. Stress–strain data of the whole triaxial test process were collected in real time using a GDSLAB system with an interval of 10 s. The tangent modulus test value at $T_1$ was obtained by dividing the deviatoric stress difference between $T_1$ and $T_2$ by the corresponding axial strain difference. Figures 13–15 show comparisons between the theoretical values of the unloading constitutive tangent modulus of the expansive clay and the test values of CTC, RTC, and RTE, respectively.

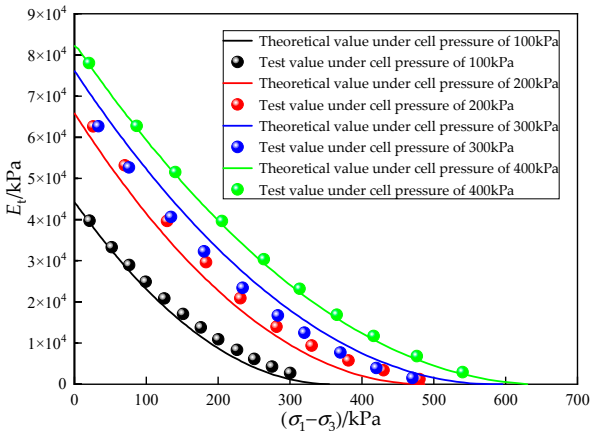


**Figure 13.** Comparison between predicted curve of tangent modulus of unified model and test value under CTC stress path.

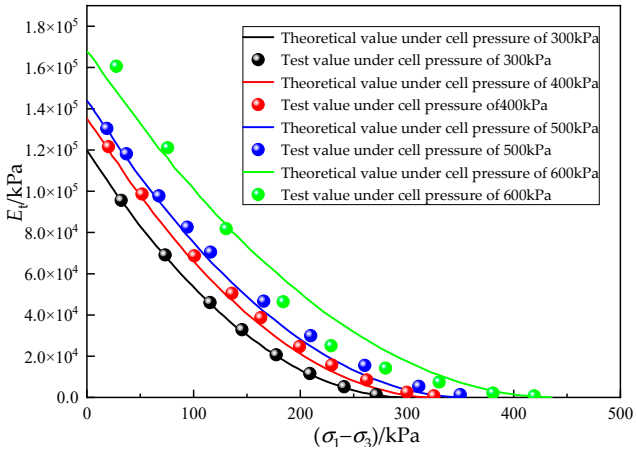


**Figure 14.** Comparison between predicted curve of tangent modulus of unified model and test value under RTC stress path.

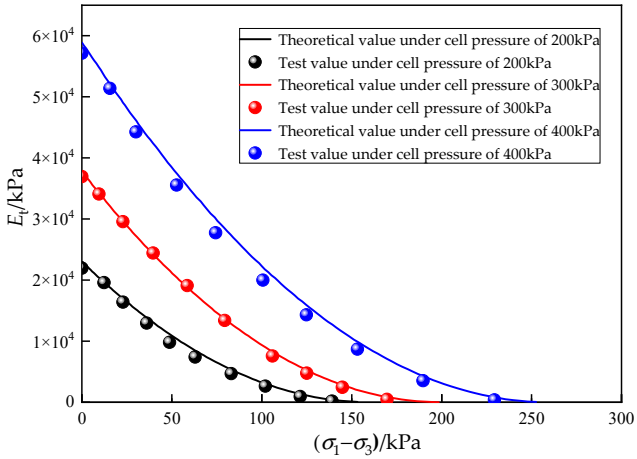


**Figure 15.** Comparison between predicted curve of tangent modulus of unified model and test value under RTE stress path.

According to the comparative analysis results in Figures 13–15, the theoretical calculation formula for the unloading constitutive tangent modulus of expansive clay based on the M-C criterion, D-P criterion, and extended SMP criterion had high prediction accuracy for the tangent modulus of the Hefei expansive clay. The error between the theoretical value and the tangent modulus value measured through the triaxial test was small, so

the theoretical formula for the tangent modulus is reasonable. Under the RTE unloading path, the error between the prediction formula based on the extended SMP criterion and the test value was less than 5%. The prediction effect was excellent. Therefore, when carrying out unloading engineering construction and design in the expansive-clay layer, the unloading constitutive model of expansive clay constructed in this paper can meet the requirements of engineering calculation accuracy. It can provide important theoretical support for foundation pit structure design and safety analysis.

## 7. Conclusions

In this study, typical expansive clay in the Hefei area was taken as the research object. A triaxial test of the unloading stress path was carried out using an automatic environmental triaxial test system (ETAS). The stress–strain properties, failure mode, and strength index of the expansive clay under the unloading stress path were explored. Through an applicability analysis of several classical soil strength criteria, an unloading constitutive model and an unloading tangent modulus expression of expansive clay were constructed based on the M-C criterion, D-P criterion, and extended SMP criterion theoretical frameworks. The following results were obtained:

(1) The stress–strain curves of the three stress paths of the expansive clay were hyperbolic, with typical strain-hardening properties. They belonged to processed hardened soil. The initial tangent modulus of the three soils increased with an increase in the initial consolidation cell pressure. The strain of the samples under lateral unloading and axial unloading lagged behind the increase in deviatoric stress, and the stress–strain curves increased sharply.

(2) Under the unloading stress path, the soil particles were involved in the unloading process of stress release. The failure samples of soil sheet elements showed obvious stretching, curling, and slipping phenomena. In terms of failure properties, CTC showed spindle-like swelling failure; RTC showed shear, splitting, and swelling failure with an increase in cell pressure; and RTE showed dumbbell-shaped necking failure.

(3) The strength of the expansive clay was significantly reduced under the unloading stress path. In the RTC path, the $c$ of the expansive clay was reduced by 32.7% compared with the CTC path, and $\varphi$ increased by 19%. In the RTE path, $c$ was reduced by 63.5% and the $\varphi$ was reduced by 28.7%.

(4) In the applicability analysis of the four classical criteria, by comparing the predicted value of failure shear stress ($q_f$) with the test value, it was found that the M-C strength criterion was suitable for the CTC stress path, while the D-P strength criterion was suitable for the RTC stress path. The generalized Tresca strength criterion was not suitable. By comparing the calculated value of the extended SMP criterion ($\tau_8$) with the calculated value of octahedral shear stress ($\tau_{8SMP}$) from the measured results, it was found that the error was less than 6%. The extended SMP criterion had an excellent effect on predicting the failure strength of the RTE path.

(5) The traditional Duncan–Chang model had obvious limitations in describing the mechanical behavior of the expansive clay under the RTC and RTE paths. The unloading constitutive model based on the D-P strength criterion and the extended SMP strength criterion could accurately predict the tangent modulus of the expansive clay under the unloading stress path. This verified the reliability of the unloading constitutive model of expansive clay.

**Author Contributions:** Conceptualization, S.P. and H.C.; methodology, S.P.; validation, Y.X. and T.Z.; formal analysis, Z.L.;writing—original draft preparation, Y.X. and T.Z.; Writing—review & editing, S.P. and G.C. All authors have read and agreed to the published version of the manuscript.

**Funding:** This research was funded by the National Natural Science Foundation of China (No. 52004003, 51878005, 51874005); and the Open Fund of Anhui Province Key Laboratory of Building Structure and Underground Engineering, Anhui Jianzhu University (No. KLBSUE-2023-06); and

the Open Project Program Foundation of the Engineering Research Center of underground mine construction, Ministry of Education (Nos. JYBGCZX2021101, JYBGCZX2020102).

**Data Availability Statement:** The datasets generated and analyzed during the current study are available from the corresponding author upon reasonable request.

**Conflicts of Interest:** The authors declare no conflicts of interest.

## References


1. Kuo, C.C.; Nelson, J.D. Validation of foundation design method on expansive soils. *Geotech. Eng.* **2019**, *50*, 103–111.
2. Lan, T.; Zhang, R.; Yang, B.Y.; Meng, X. Influence of swelling on shear strength of expansive soil and slope stability. *Front. Earth Sci.* **2022**, *10*, 849046. [CrossRef]
3. Lu, T.S.; He, H.; Liu, S.Y.; Yang, J.; Li, C.; Feng, M. SCPTU-based numerical analyses of an excavation in soft clay. *Chin. Civ. Eng. J.* **2023**, *56*, 141–148.
4. Gao, Z.A.; Kong, L.W.; Wang, S.J. Deformation behavior and shear zone evolution characteristics of undisturbed expansive soil with different fissure directions under plane strain condition. *Rock Soil Mech.* **2023**, *44*, 2495–2508.
5. Li, L.; Zang, M.; Zhang, R.T.; Lu, H.J. Experimental Study on Mechanical Properties of Structured Clay under Different Unloading Rates and Unloading Stress Paths. *Buildings* **2023**, *13*, 1544. [CrossRef]
6. *GB 50112-2013*; Ministry of Housing and Urban-Rural Development of the People's Republic of China. Technical Code for Building in Expansive Soil Area. China Building Industry Press: Beijing, China, 2013.
7. Huang, W.; Li, J.; Lu, Y.; Li, D.; Mou, Y.; Wu, X.; Jiang, Z.; Li, Z. Mechanical properties of soft soil considering the influence of unloading stress paths. *Adv. Civ. Eng.* **2021**, *2021*, 8813882. [CrossRef]
8. Yang, Y.; Lin, J.; Wu, Y.; Peng, S.; Shao, W.; Yang, L. Energy characteristics of saturated Jurassic sandstone in western China under different stress paths. *Deep. Undergr. Sci. Eng.* **2024**, 1–11. [CrossRef]
9. Lambe, T.W. Stress Path Method. *J. Soil Mech. Found. Div.* **1967**, *93*, 309–331. [CrossRef]
10. Duncan, J.M.; Chang, C.Y. Nonlinear Analysis of Stress and Strain in Soils. *J. Soil Mech. Found. Div.* **1970**, *96*, 1629–1653. [CrossRef]
11. Gao, Z.Z.; Hu, D.X.; Zhang, Q.Y. Study on constitutive model of soil under complex stress path. *Adv. Eng. Sci.* **1997**, *1*, 50–56.
12. Ying, D.S.; Wang, B.T.; Wang, Y.T. Tangent elastic modulus of Duncan-Chang model for different stress paths. *Chin. J. Geotech. Eng.* **2007**, *9*, 1380–1385.
13. Goto, S.; Burland, J.B.; Tatsuoka, F. Non-linear soil model with various strain levels and its application to axisymmetric excavation problem. *Soil Found.* **1999**, *39*, 111–119. [CrossRef] [PubMed]
14. Roscoe, K.H.; Schofield, A.N.; Thurairajah, A. Yielding of clay in states wetter than critical. *Geotechnique* **1963**, *13*, 211–240. [CrossRef]
15. Ma, P.C.; Ke, H.; Tong, X. Nonlinear constitutive model of soil–bentonite based on triaxial tests along different stress paths. *Can. Geotech. J.* **2021**, *58*, 682–694. [CrossRef]
16. Roscoe, K.H.; Burland, J.B. *On the Generalised Stress-Strain Behavior of "Wet" Clay*; Cambridge University Press: Cambridge, UK, 1968; pp. 535–609.
17. Robert, S.C.; Kenneth, L.I. Response of granular soil along constant stress increment ratio path. *J. Geotech. Eng.* **1990**, *116*, 355–376. [CrossRef]
18. Matsuoka, H.; Yao, Y.; Sun, D. The Cam-clay models revised by the SMP criterion. *Soils Found.* **1999**, *39*, 81–95. [CrossRef]
19. Sun, D.A.; Yao, Y.P.; Yin, Z.Z. Generalization of elasto-plastic model with two yield surfaces based on SMP criterion. *Chin. J. Geotech. Eng.* **1999**, *21*, 631–634.
20. Yao, Y.P.; Wang, N.B. Unified hardening equation for soils in complex stress paths. *Chin. J. Rock Mech. Eng.* **2023**, *42*, 2041–2047.
21. Zou, B.; Yao, Y.P.; Lu, D.C. Qinghua model revised by SMP criterion. *Chin. J. Rock Mech. Eng.* **2005**, *24*, 4303–4307.
22. Lu, D.C. A constitutive model for soils considering stress paths based on generalized nonlinear strength theory. *Chin. J. Rock Mech. Eng.* **2007**, *26*, 1512.
23. Zhang, K.Y.; Zang, Z.J.; Li, W.; Wen, D.B.; Nai, C.F. Three-dimensional elastoplastic model of soil with consideration of unloading stress path and its experimental verification. *Rock Soil Mech.* **2019**, *40*, 1313–1323.
24. Yin, X.; Li, M.; Xia, B.; Shen, N.; Jiang, G.; Zhong, J. Shear behavior of saturated silt under complex unloading paths. *Chin. J. Geotech. Eng.* **2023**, *45*, 75–78.
25. Qiu, Y.; Ding, W.; Zhao, T.; Wang, X.; Qiao, Y. Asymmetrical deformation characteristics and mechanisms of deep excavations induced by one-side unloading. *Chin. J. Geotech. Eng.* **2024**, *46*, 199–206.
26. Li, F.G.; Ji, R.H.; Wang, X.M. *Investigation and Evaluation of Disaster-Causing Special Soil in Anhui Province*; Anhui Province Geological Prospecting Bureau Second Hydrological Engineering Geology Survey Institute: Wuhu, China, 2008.
27. *GB/T 50123-2019*; Standard for Geotechnical Test Methods. Standardization Administration of the People's Republic of China: Beijing, China, 2019.
28. Zhang, T.; Peng, S.L.; Cao, G.Y.; Zhang, Y.J. Experimental study on expansive soil lateral unloading and analysis on its normalized characteristics. *Water Resour. Hydropower Eng.* **2023**, *54*, 175–186.
29. Li, X.; Jia, Y.; Wang, Z.; Sun, Y.; Yin, S. Step-changed strain rate effect on the mechanical properties of undisturbed expansive clay. *Eur. J. Environ. Civ. Eng.* **2024**, *28*, 38–52. [CrossRef]

30. Yu, M.H.; Peng, Y.J. Advances in strength theories for materials under complex stress state in the 20th century. *Adv. Mech.* **2004**, *34*, 529–560. [CrossRef]
31. Cai, M.F. *Rock Mechanics and Engineering*; Science Press: Beijing, China, 2013.
32. Matusoka, H. Prediction of plane strain strength for soils from triaxial compression. In Proceedings of the 10th International Conference on soil Mechanics and Foundation Engineering, Stockholm, Sweden, 15–19 June 1981; Volume 5, pp. 682–683.
33. He, S.X.; Long, L.H.; Yang, X.Q.; He, Y. Experimental study of yield property of clayey soil under unloading. *Rock Soil Mech.* **2008**, *29*, 449–452.
34. Li, J.J.; Kong, L.W.; Jin, L. Stress history and time effect on shear modulus of expansive soils. *Arab. J. Geosci.* **2022**, *15*, 35. [CrossRef]
35. Kondner, R.L. Hyperbolic stress-strain response: Cohesive soils. *J. Soil Mech. Found. Div.* **1963**, *89*, 115–143. [CrossRef]
36. Shao, D.C. A modified duncan-chang model and its application to numerical simulation of earth-rock dam. *China Three Gorges Univ. (Nat. Sci.)* **2015**, *37*, 21–24.